Estimation of the hydraulic conductivity of saturated sand-marine clay mixtures with a homogenization approach

by

X.S. Shi
Department of Civil and Environmental Engineering,
The Hong Kong Polytechnic University, Hung Hom, Kowloon, Hong Kong.
Email: xsshi@polyu.edu.hk

Jianhua YIN
Department of Civil and Environmental Engineering
The Hong Kong Polytechnic University, Hung Hom, Kowloon, Hong Kong, China
Tel: (852) 2766-6065, Fax: (852) 2334-6389, Email: cejhyin@polyu.edu.hk

June 2017

Abstract

A series of oedometer tests was performed on a pure marine clay and sand-marine clay mixtures with various initial water contents of the clay matrix and sand fractions. The hydraulic conductivity was computed from the compressibility and the consolidation curves of the samples. The experimental data indicate that the overall hydraulic conductivity of the mixtures depends on both the initial water content and sand fraction of the clay matrix at a given stress level. The initial water content of the clay matrix has an influence on the local void ratio, leading to differences in the overall hydraulic conductivity. The influence of the initial water content is substantially reduced in case of the relationship between the overall hydraulic conductivity and the overall void ratio. A homogenization approach is introduced in this paper to estimate the overall hydraulic conductivity which can be determined from the intrinsic permeability parameters of the pure marine clay. The proposed model has four parameters, including two intrinsic parameters of the pure marine clay and two additional ones incorporating the evolution of sand skeleton. The ability of the proposed model to describe the permeability behavior of the sand-marine clay mixtures (and other sand-clay mixtures from literature) is verified by using test data.

Keywords: Hydraulic conductivity; Sand-clay mixtures; Sand fraction; Initial water content; Marine clay

1. Introduction

Sand clay mixtures may be produced in land reclamation, marine deposit improvement (e.g., Silva, 2016) or degradation of natural materials (Zhou *et al.*, 2017). In previous literature, most of the researchers focused on the hydraulic conductivity of sand-clay mixtures which are used in waste disposal facilities (Pandian *et al.*, 1995; Sivapullaiah *et al.*, 2000) and dredging engineering (Deng *et al.*, 2016). Additionally, mixtures consisting of sand (or rock particles) and natural soils (as clay matrix) were also investigated (e.g., Watabe *et al.*, 2011; Elkady *et al.*, 2015; Barla and Beer, 2012; Zhou *et al.*, 2017). The sand-clay mixture has a similar structure to other binary mixtures, e.g., asphalt mixture (Huang, *et al.*, 2016; Zhang and Yang, 2017) and sand-tire chip mixture (Mashiri, *et al.*, 2016) which are widely used in pavement design and other civil engineering projects. This type of binary mixture consists of a soft matrix and incompressible inclusions. Supposing that stiff inclusions are randomly distributed within a soft matrix. In this case, the skeleton of the inclusions governing the mechanical and permeability properties depends on the volume fraction of the inclusions.

The effect of coarse sand fraction on the overall hydraulic conductivity was well documented and the following words can be made referring to the previous work.

(1) The overall hydraulic conductivity depends on the clay matrix for a lower sand fraction. With increase of the sand fraction, a granular skeleton gradually forms, and the overall conductivity was governed by the intergranular sand structure.

(2) After being normalized by the liquid limit, the overall hydraulic conductivity vs. overall void ratio shows approximately a unique relationship which is consistent with that of the pure clay.

(3) The overall hydraulic conductivity of a sand-clay mixture is higher than that of the corresponding pure clay at a given stress level.

(4) The particle size and type of the coarse inclusions affects the overall hydraulic

conductivity: a mixture with coarse sand gives a higher hydraulic conductivity than that containing fine sand.

The mentioned work provides useful information for further study. Based on laboratory data, some researchers proposed equations for the estimation of hydraulic conductivity of sand-clay mixtures (e.g., Pandian *et al.*, 1995; Sivapullaiah *et al.*, 2000; Deng *et al.*, 2017). Most of them were based on the regression analysis, relating the hydraulic conductivity to the overall void ratio and the corresponding liquid limit. Some researchers try to study the structure transition of the mixtures with increasing sand fraction (Graham *et al*., 1989; Mitchell, 1993; Thevanayagam and Mohan, 1998; Chu and Leong, 2002; Monkul and Ozden, 2005). In their analysis, the sand-clay mixture was idealized as a two-phase composite material in which clay is the matrix and sand particles represent the inclusions. In this case, the evolution of clay void ratio (void ratio of clay matrix) and skeletal void ratio (defined as the ratio of the volume of clay matrix to the volume of sand particles) was computed, and their relationship relating to the overall hydraulic conductivity was analyzed. However, the mechanisms governing the change of hydraulic conductivity (especially the evolution of local hydraulic conductivity of the clay matrix, and its relationship with the overall hydraulic conductivity) was still not well understood, and a simple but effective model considering the evolution of sand skeleton needs to be proposed.

In most of the previous literatures, a permeability test on a pure clay was performed as a reference. However, its initial water content is usually not the same as that of the clay matrix in sand-clay mixtures. It is well recognized that the compression behavior of remolded clays is affected by the initial water content (e.g., Cerato and Lutenegger, 2004; Hong *et al*., 2010; Shi and Herle, 2015; Zeng *et al.*, 2015; Zeng *et al.*, 2016; Tsuchida, 2017). Hence, the void ratio of the clay matrix in a mixture (with the same sand fraction but different initial water content of the clay matrix) should be different at a given stress level, which would affect the overall hydraulic conductivity. But the effect of initial water content on the overall hydraulic conductivity of sand-clay mixtures has been seldom investigated. In this study, sand-marine clay mixtures with different initial water contents and different sand fractions are performed, and a simple theoretical model is proposed within the homogenization framework for estimating the overall hydraulic conductivity.

2. Materials and methods

The materials include a coarse sand material and a clayey soil from Hong Kong Marine Deposits (HKMD). The basic physical properties of the tested soils are given in Table 1 (according to BS1377). The maximum void ratio of the sand is 0.945, and the corresponding minimum value is 0.601.

Since the produced clay slurry has a high initial water content (higher than 2.0 times the liquid limit), it was exposed to air for a couple of days to reduce its moisture. Afterwards, water was added to the samples to reach four desired water contents[1] for producing the mixtures:67.9%, 74.5%, 86.9% and 99.5%, respectively. The adopted sand fraction ψ_s (defined as the dry mass ratio of the sands to a mixture) is lower than 60% (four different sand mass fractions are considered: 0%, 20%, 40%, 60%), since a higher sand fraction may lead to micro air bubbles in a mixture. The samples were mixed carefully to make it uniform. Then, the mixtures were put in an airtight container for a period of time to get a high degree of saturation.

A filter paper was placed on a porous stone to prevent loss of fine particles. Afterwards, the consolidation ring (diameter =7.00 cm, height =1.90 cm) was placed on the porous stone.

[1] Segregation may happen in case of a high initial water content of the clay matrix. In this case, the settlement of sand inclusions is faster than that of the marine clay particles. However, a notable segregation happens only if the clay matrix has an initial water content higher than 5.0 times liquid limit (Tan *et al.*, 1990; Sridharan and Prakash, 2003). The initial water contents of the clay matrix are below 1.60 times the liquid limit. Therefore, the segregation effect may be neglected.

The sand-clay mixtures were spooned into a consolidation ring up to the height of the ring, followed by placing a filter paper on the top of the sample. Finally, a loading cap with a porous bottom was placed above the upper filter paper, which corresponds to an initial consolidation stress of 1.7 kPa. After being fixed in the loading frame, a subsequent stress of 2.5 kPa was applied to prevent soil squeezing between the consolidation ring and the loading cap. The consolidation stress was then increased stepwise (5, 10, 25, 50, 100, 200, 400, 800 and 1200 kPa). The duration of every load increment was determined according to the corresponding consolidation curves at a given total stress level.

3. State variables

Given that the sand inclusions are randomly arranged in the marine clay matrix which is semi-homogeneous on a macro-scale. In this case, both local and overall variables can be easily defined and computed from laboratory data. Some assumptions are made as follows: (1) the mixture is assumed to be saturated, with no air bubbles in the clay matrix or on the clay-sand particle interface[2]; (2) Since the sand inclusions (not the sand skeleton) are much stiffer than the clay matrix, they are assumed to be incompressible (e.g., Monkul and Ozden, 2005); (3) The sand inclusions are impermeable, and all moisture is associated with the marine clay matrix (e.g., Mitchell, 1993).

Based on the above assumptions, a sand-clay mixture can be divided into three parts: the volume of sand inclusions V_{ss} (cm^3), the void part V_v (cm^3) and solid part V_{sc} (cm^3) in the marine clay matrix. In this paper, the authors choose the volume fraction of sand particles as a structure variable:

[2] This is not suitable for a sand-clay mixture with a relatively high sand fraction, in which the clay matrix is not enough to fill the inter-granular spaces (Sivapullaiah *et al.*, 2000; Watabe *et al.*, 2011).

$$\phi_s = \frac{V_{ss}}{V_v + V_{sc} + V_{ss}} \tag{1}$$

Considering that the sand particles are incompressible (Assumption 1), ϕ_s can be computed from the local void ratio e_c (void ratio of the clay matrix) and the corresponding overall value e (overall void ratio of sand-clay mixtures):

$$\phi_s = \frac{e_c - e}{e_c + ee_c} \tag{2}$$

with the local void ratio $e_c = \frac{V_v}{V_{sc}}$, and overall void ratios $e = \frac{V_v}{V_{sc} + V_{ss}}$. Considering that the mixture is saturated (Assumption 2), the sand inclusions are impermeable, and all moisture is associated with the marine clay matrix (Assumption 3) within the test stress range, the void ratio of the clay matrix is given as

$$e_c = \frac{e\rho_c}{(1 - \psi_s)\rho} \tag{3}$$

Where ρ_c (g/cm^3) is the density of soil particles in clay matrix, and ρ (g/cm^3) is the overall particle density of a sand-clay mixture. From the conservation of the volumes and masses of the clay matrix and sand inclusions, the overall particle density of sand-clay mixtures ρ (g/cm^3) is derived as

$$\rho = \frac{\rho_c \rho_s}{(1 - \psi_s)\rho_s + \psi_s \rho_c} \tag{4}$$

where ρ_s (g/cm^3) is the density of sand particles. The overall void ratio e in Eq. (3) is related to the current overall strain ε (logarithmic strain was used in this study for a large strain of the mixture samples in oedometer tests) and the initial overall void ratio e_0:

$$e = (1 + e_0)\exp(-\varepsilon) - 1 \tag{5}$$

Substitution of Eqs (4) and (5) into Eq. (3), one computes the local volumetric variable e_c. Furthermore, one can get the state variable ϕ_s from Eq. (2). Note that the current vertical strain

ε can be calculated from the initial height of a sample and the settlement at an incremental stress level. Significant difference in stiffness of the constituents leads to a non-uniform stress distribution (Harshin, 1983; Shi & Herle, 2017; Jamei, *et al.*, 2013; Zhuang *et al.*, 2017). To this end, the volume average stresses are used, with σ' (kPa) and σ'_c (kPa) denoting the overall effective stress and the local effective stress in the clay matrix, respectively.

4. Test results and discussions

Given the definition of variables (stresses, strains, void ratios and porosities), the test data can be analyzed. The saturated hydraulic conductivity is derived from the oedometer compression data. The definition of coefficient of consolidation (cm^2/s) is

$$c_v = \frac{k}{\gamma_w}\frac{\mathrm{d}\sigma'}{\mathrm{d}\varepsilon} = -\frac{k}{\gamma_w}\frac{\mathrm{d}\sigma'}{\mathrm{d}(\ln(1+e))} \tag{6}$$

Herein, k (cm/s) denotes the hydraulic conductivity; γ_w ($\mathrm{g/s^2/cm^2}$) is the unit weight of water. A double logarithmic $\ln\sigma'$-$\ln(1+e)$ relationship (Butterfield, 1979) can well represent the compression curves of sand-marine clay mixtures (see Appendix, Figs a-d):

$$\ln(1+e) = N - \lambda\ln(\sigma'/\sigma'_r) \tag{7}$$

where σ'_r=1 kPa is a reference stress, N and λ are parameters (N corresponding to the reference stress, and λ being the slope of the Normal Compression Line in double logarithmic plot). The above equation can well fit the compression curve of various remolded soils (e.g., Sridharan & Prakash, 1996; Hong & Onitsuka, 1998; Hong *et al.*, 2010; Shi & Herle, 2015). Combining Eqs (6) and (7), the coefficient of consolidation can be expressed as

$$c_v = -\frac{k}{\gamma_w}\frac{\mathrm{d}(\ln\sigma')}{\mathrm{d}(\ln(1+e))}\sigma' = \frac{k\sigma'}{\gamma_w\lambda} \tag{8}$$

From Eq. (8), one derives the overall hydraulic conductivity:

$$k = \frac{\lambda c_v \lambda_w}{\sigma'} \tag{9}$$

c_v=0.212h^2/t_{90}, t_{90} (s) is the time duration at 90% of consolidation, and h (cm) is the height of the specimen.

The computed data for the sand-marine clay mixtures are shown in Fig. 1 in terms of overall hydraulic conductivity and overall effective stress on a double-logarithmic (lnσ'-ln$k$) scale. It is seen that the difference of hydraulic conductivity (mixtures with different sand fractions) is not significant within 25 kPa, which becomes distinct with increasing stress at a given initial water content. Additionally, the results suggest that the overall hydraulic conductivity increases with the increase of sand fraction beyond 25 kPa.

The influence of initial water content of the clay matrix on the overall hydraulic conductivity is shown in Fig. 2 (lnσ'-ln$k$ plot). In general, the (overall) hydraulic conductivity for a higher initial water content is higher than that for a lower one. Regarding the pure marine clay, the compression curve is not unique (see Appendix, Fig. a): a sample with a higher initial water content possesses a higher void ratio at a given stress level (Cerato & Lutenegger, 2004; Hong *et al.*, 2010; Shi & Herle, 2015; Bian *et al.*, 2016; Bian *et al.*, 2017), leading to different value of hydraulic conductivity. Analogously, the compression curve of the mixtures is also affected by the initial water content of the clay matrix (see Appendix, Figs b-d). In this case, a higher overall void ratio (corresponding to a higher initial water content of the clay matrix) induces a higher value of overall hydraulic conductivity (see Fig. 2).

The properties of clay matrix are usually a frame of reference for interpreting the overall behavior of sand-clay mixtures in different states. After being plotted in terms of hydraulic conductivity and void ratio on a double-logarithmic (lne_c-lnk_c) scale (Fig. 3a), the influence of initial water content on the permeability of the pure marine clay seems to be negligible. It is seen that there is approximately a linear relationship between lne_c and lnk_c:

$$\ln(k_c/k_r) = A_c + \xi_c \ln e_c \tag{10}$$

Where k_r =1 cm/s is a reference permeability, ξ_c is the slope of the fitting line in $\ln e_c$:$\ln k_c$ plane, and A_c corresponds to a reference void ratio e_c=1. The power relationship between k_c and e_c was proposed by Mesri & Olson (1971) describing the permeability for a remolded soil. This corresponds to the findings in previous work by other researchers (e.g., Carrier & Beckman, 1984; Zeng *et al.*, 2011, Zeng *et al.*, 2012).

The ln$e$-ln$k$ relationship for sand-marine clay mixtures is shown in Fig. 3b. The overall hydraulic conductivity of a sand-clay mixture increases with increasing sand fraction at a given overall void ratio, which is consistent with the data from literature (e.g., Pandian *et al.*, 1995; Watabe *et al.*, 2011). The hydraulic conductivity for sand-clay mixtures are not well in line with the pure marine clay (Fig. 3a), especially for a sand fraction of 60%. This may be induced by the evolution of sand skeleton with increasing sand fraction.

Combining Eqs (3) - (5), one calculates the local void ratio e_c. Data of local void ratio vs. the overall hydraulic conductivity are gathered in Fig. 4. It is clear that the influence of sand fraction is significantly reduced after introducing the local void ratio of the clay matrix.

5. Estimation of overall hydraulic conductivity for sand-clay mixtures

Classical homogenization techniques were proposed following the mean-field homogenization scheme (Hill, 1965; Mori and Tanaka, 1973; Lielens *et al.*, 1998). Homogenization laws were derived through averaging techniques within the Representative Elementary Volume (RVE) concept (Eshelby, 1957). RVE should represent the microstructure containing statistically sufficient mechanisms (Gonzalez *et al.*, 2004; Quayum *et al.*, 2015; Zhuang *et al.*, 2015). The homogenization approaches were widely used in (Thermo-)Hydro-Mechanical analysis of multi-phase materials (Zhuang *et al.*, 2014; Shi *et al.*, 2017), complex crack propagation (Budarapu *et al.*, 2014; Talebi *et al.*, 2014), thermal conductivity of polymer reinforced composites (He *et al.*, 2016). In this section, the homogenization law would be derived from analyzing the intergranular structure evolution of sand-clay mixtures.

5.1 Homogenization

From the homogenization concept, the structure of sand-clay mixtures can be bounded by two limit configurations: (1) the hydraulic conductivity is the highest (upper bound) if the sand and clay matrix are ranged in parallel in the water flow direction (parallel structure), and (2) the hydraulic conductivity approaches the lower bound when the constituents are in series in the flux direction. From the process of producing sand-clay mixtures, the sand inclusions can be assumed to be randomly distributed in the reconstituted constituent. Consequently, the parallel and series configurations are of equivalent effect on the overall behavior. Analogous to the analysis of the effective stiffness of composite soils (Shi and Herle, 2017), the logarithm of the overall hydraulic conductivity can be approximated by the volume average values of the constituents.

Considering that the sand inclusions are approximately impermeable. In this case, the overall hydraulic conductivity only depends on the clay matrix (denoted as 'saturation state' of a composite material by Tu *et al.*, 2015). Furthermore, the mentioned 'volume average approximation' can only reproduce the overall behavior with a good accuracy at low coarse fractions, e.g., with no direct contacts between the sand inclusions. With increase of the sand fraction, possible force chains linking the sand particles form, which induces a gradual transition to the parallel configuration (Tu *et al.*, 2015). To this end, a relationship governing the evolution of sand skeleton is given as

$$\ln k = \eta(1 - \phi_s)\ln k_c \tag{11}$$

Where η is a structure variable related to the inter-granular structure evolution of the sand skeleton in sand-clay mixtures. If the sand inclusions are randomly distributed in the soft clay matrix, η depends on the volume fraction of sand inclusions. For a given stress level, the structure variable can be computed from the local and overall hydraulic conductivities of sand-clay mixtures. In the sequel, the evolution of structure parameter will be presented and analyzed.

5.2 Local hydraulic conductivity and evolution of structure parameter

Thanks to the incompressible sand particles, the void ratio of the clay matrix is computed, and its relationship with the overall stress is summarized in Fig. 5. At a given overall stress level, the local void ratios of the clay matrix are e_{c1} (20% sand fraction), e_{c2} (40% sand fraction) and e_{c3} (60% sand fraction), with $e_{c1}<e_{c2}<e_{c3}$. The local hydraulic conductivity represents the hydraulic conductivity of the clay matrix. If it is assumed that the hydraulic conductivity of the clay matrix in sand-clay mixtures is consistent with that of the pure clay. At a given overall stress level, the local hydraulic conductivity depends on the overall void ratio. Substitution of Eq. (3) into Eq. (10) gives

$$\ln(k_c/k_r) = A_c + \xi_c \ln\left(\frac{\rho_c}{(1-\psi_s)\rho}\right) + \xi_c \ln e \tag{12}$$

As can be seen in Fig. 5, at a given stress level, the values of local hydraulic conductivity are k_{c1} (20% sand fraction), k_{c2} (40% sand fraction) and k_{c3} (60% sand fraction), with $k_{c1}<k_{c2}<k_{c3}$. This provides an explanation to the fact that the overall hydraulic conductivity increases with the sand fraction (Fig. 1).

The evolution of the structure variable η is shown in Fig. 6. It is seen that η increases with increasing overall effective stress, and the value with a higher sand fraction lies above the one with a lower sand fraction. The change of η resembles that of the volume fraction of the sand particles, suggesting a possible relationship between these two state variables.

Fig. 7 shows the relationship between the structure variable and the volume fraction of the sand particles: the structure variable increases with the increasing volume fraction of sand, which shows a slightly nonlinear relationship. One may imagine two limit cases: a negligible sand fraction ϕ_s=0 and an upper bound of the sand fraction ϕ_s=α. From Eqs (3) and (4), the void ratio of the clay matrix is overall value in case of ϕ_s=0, and the corresponding structure variable is reduced to one. Note that the upper bound of sand fraction α is not necessarily the same as the one measured according to BS1377. It is a stress dependent variable which can be reached by means of cyclic shearing with small amplitude (Herle and Gudehus, 1999). The structure variable at the upper bound of sand fraction can be determined from analysis of the local variables.

The overall deformation process follows the clay matrix due to the incompressible sand particles. Therefore, the local coefficient of consolidation is the same as the overall value c_v. Analogous to the derivation of the overall hydraulic conductivity (Eq. (9)), the local value can be given as

$$k_c = \frac{\lambda_c c_v \lambda_w}{\sigma'_c} \tag{13}$$

For a sand-clay mixture with the upper bound of sand fraction, the sand skeleton has to overtake an extra incremental stress alone. Given a stress increment, the local variables (e.g., the local compression coefficient λ_c, local stress σ'_c and coefficient of consolidation c_v) remain unchanged. In this case, the local hydraulic conductivity k_c is a constant. However, the overall compression coefficient λ is approximately zero due to the stiff sand skeleton, leading to an infinitesimal overall hydraulic conductivity (Eq. (9)). Consequently, the structure variable satisfies

$$\frac{\ln k}{\ln k_c} = \infty \tag{14}$$

An equation satisfying the above limit cases is given as

$$\eta = \left(\frac{\alpha}{\alpha - \phi_s} \right)^{\beta} \tag{15}$$

where α corresponding to an upper bound of the volume fraction of sand particles, and β is a structure parameter. The homogenization approach (Eqs (11) and (15)) is simple with fewer parameters compared with homogenization models in previous literatures. It may have penitential application for engineers in geotechnical engineering.

Now a full model is proposed for the estimation of remolded sand-marine clay mixtures, with a general procedure as follows: First, the local void ratio e_c was computed from Eqs (3) and (4), and the volume fraction of sand particles ϕ_s was subsequently determined; Then, the structure variable η is calculated by Eq. (15); Finally, the overall hydraulic conductivity can be computed by substituting Eq. (12) into Eq. (11).

6. Validation of the proposed model

There are four parameters in the proposed model: A_c, ξ_c, α and β. A_c and ξ_c are intrinsic permeability parameters corresponding to the pure clay matrix, and they are not sensitive to the initial water content; α and β are structure parameters representing the evolution of sand skeleton for a sand-clay mixture. At least two oedometer (or falling head hydraulic conductivity) tests are needed for the calibration of model parameters: one test on the pure marine clay and the other one on a sand-clay mixture with a specified sand fraction, to calibrate the intrinsic permeability parameters and inter-granular structure parameters, respectively. In this section, the model predictions will be compared with the laboratory data and the data from literature. The model parameters for the sand-marine clay mixtures (and other sand-clay mixtures) are listed in Table 2.

6.1 Sand-marine clay (HKMD) mixtures

The validity of the proposed model is first evaluated by comparing the test data of the sand-marine clay mixtures with the model proposed in the last section. The corresponding model parameters are listed in Table 2. The predicted compression curves are shown in Fig. 8 together with the experimental data. It can be seen that the hydraulic conductivity of the sand-marine clay mixtures can be well reproduced by the model except for the tests with an initial water content of the matrix of 99.5% (a slight difference). A possible explanation may be given as follows: increasing the initial water content reduces the electrolyte concentration in the marine clay matrix, which tends to reduce the coefficient of permeability (Mesri and Olson, 1971). Since the electrolyte concentration are within a narrow range for the tested soil, only the hydraulic conductivity of the pure clay at very high initial water content shows a slight deviation. If a new set of parameters (fitting from the pure marine clay with an initial water content of 99.5%) is adopted (Nc=18.51 and λc=4.52), the experimental data and model prediction would be more consistent. However, it is suggested to use the original values of the intrinsic parameters (N_c=18.25 and λ_c=4.35), since it reduces the number of model parameters, and the errors in Fig. 8(d) are acceptable in geotechnical point of view.

6.2 Sand-clay mixtures from literature

The model was proposed based on the tests for the sand-marine clay mixtures. Its capability on other sand-clay mixtures will be evaluated in this section.

(1) A sand-bentonite mixture

The experimental data carried out by Pandian *et al.* (1995) have been compared with the model predictions. The bentonite clay matrix was from the Kolar district in Karnataka state, India. It has a liquid limit of 330% and a plastic limit of 70%. The particle size of the sand particles varies between 0.075 mm and 0.425 mm. Two different sand fractions were considered: 41% and 51%. The hydraulic conductivity was measured using falling head hydraulic conductivity tests at various equilibrium pressures during oedometer tests. The calibrated model parameters are given in Table 2 (The calibration of structure parameter is shown in Fig. 9. Comparisons between the experimental data and theoretical simulations are shown in Fig. 10. It can be seen that the behavior of sand-bentonite mixtures has been simulated satisfactorily with the proposed model.

(2) Sand-bentonite-kaolin mixtures

Results of the experimental work performed by Deng *et al.* (2017) are used for the validation of the model. The clay matrix was a mixture of kaolin and bentonite. Three sets of tests considering different dry mass ratios of bentonite to kaolin (9/1, 7/3 and 5/5) were reported. Each set of tests includes three different sand fractions (30%, 40%, and 50%). The size of sand particles is smaller than 1.0 mm, and the sand material has the maximum void ratio of 0.83 and the minimum void ratio of 0.485, respectively. Similar to this study, the hydraulic conductivity was estimated following Terzaghi's consolidation theory. The calibration of structure parameter is shown in Fig. 11, suggesting that the structure parameter depend on the sand materials (e.g., shape and size of sand particles), regardless of the clay matrix. It is consistent with the discussions on the structure variable in the last section. The measured and simulated hydraulic conductivity results of the mixtures are shown in Fig. 12. The proposed model can well reproduce the sand-bentonite-kaolin mixtures except for several points at very high stress levels (e.g., 1600 kPa).

(3) Other sand-clay mixtures

The experimental results performed by Sivapullaiah *et al.* (2000) on sand-bentonite mixtures and by Watabe *et al.* (2011) on sand-Nagoya clay mixtures, have been compared with the model predictions (see corresponding references for more details on the materials).

The calibrated parameters are given in Table 2. Analysis using the proposed model was performed for each of tests. In Fig. 13, the hydraulic conductivity predicted by the model for the mixtures is compared with the experimental data. Most of the data points lie on or close to the 45° line, indicating the capability of the model in predicting the hydraulic conductivity behavior of sand-clay mixtures.

Several assumptions were made for the analysis of the test data, which is discussed as follows: (1) The soil is assumed to be a binary mixture, with no macro voids in the clay matrix or on the sand clay interface. The soil sample was mixed carefully in the lab, afterwards, air bubbles in the samples were expelled by a vibration process. Furthermore, the maximum sand mass fraction is 60%, which is low enough for the clay matrix to fill the inter-granular space. (2) It is also assumed that the sand inclusions are incompressible, impermeable and all moisture is associated with the clay matrix. Since the stiffness (hydraulic conductivity) of the sand inclusions are significantly higher (lower) than that of the clay matrix. This assumption is reasonable and was adopted by many researchers (e.g., Mitchell, 1993; Kumar, 1996; Sivapullaiah, *et al.*, 2000; Monkul and Ozden, 2005).

7. Sensitivity analysis for the proposed model

A sensitivity analysis on the model parameters will be done in this section. The intrinsic permeability data of pure marine clays are well consistent (Fig.3a), which can be uniquely defined by Eq. (10), irrespective of stress levels and initial water contents of the clay matrix. Additionally, the logarithmic value of overall permeability changes linearly with that of the local value for a given volume fraction of sand inclusions (Eq. (11)). Therefore, the sensitivity analysis is done only for the structure parameters α and β.

As mentioned above, the inter-granular structure parameter α and β are calibrated from an oedometer test on sand-clay mixture with a specified sand fraction. In laboratory tests, the sand inclusions may be not perfectly distributed in the marine clay matrix. Therefore, the value of the structure parameters shows a slight oscillation. The authors have done 12 oedometer tests on the sand-marine clay mixtures. Correspondingly, 12 samples of the structure parameters can be extracted from the laboratory tests. In this study, the Weibull distribution (Weibull, 1951) was adopted for the structure parameters with probability density functions as follows:

$$f(\alpha) = \frac{m_\alpha}{\zeta_\alpha}\left(\frac{\alpha}{\zeta_\alpha}\right)^{m_\alpha - 1} \exp[-(\alpha / \zeta_\alpha)^{m_\alpha}] \tag{16a}$$

$$f(\beta) = \frac{m_\beta}{\zeta_\beta}\left(\frac{\beta}{\zeta_\beta}\right)^{m_\beta - 1} \exp[-(\beta / \zeta_\beta)^{m_\beta}] \tag{16b}$$

Where m_α=2.31 and m_β=2.06 are the shape parameters; ζ_α=0.72 and ζ_β=0.71 are the scale parameters of Weibull distribution. The calibration of parameters for Weibull distribution is given in Fig. 14. The correlation coefficients are 0.94 and 0.95 for Eq. (17a) and Eq. (17b), respectively. $\mathrm{F}(\alpha)$ and $\mathrm{F}(\beta)$ in the figure denote corresponding cumulative distribution functions.

$$\mathrm{F}(\alpha) = 1 - \exp[-(\alpha / \zeta_\alpha)^{m_\alpha}] \tag{17a}$$

$$\mathrm{F}(\beta) = 1 - \exp[-(\beta / \zeta_\beta)^{m_\beta}] \tag{17b}$$

Based on the probability density function, one creates series of random input structure parameters using Monte-Carlo method. The following state variables were adopted: e=0.82, ϕ_s=0.22, corresponding to w_{c0}=99.5% with a sand fraction of 40% (σ'=100 kPa). The overall permeability is then computed from Eqs (11), (12) and (15). The probability density of the overall hydraulic conductivity is presented in Fig. 15, and the change of average value of the overall hydraulic conductivity with the number of simulation is shown in Fig. 16. It is seen that there is an oscillation in the beginning, then it shows a statistical convergence beyond 150 times of simulation. Note that this part provides only a preliminary sensitivity analysis on the structure parameters, since the main work of this study is to give a practical approach for the estimation of overall hydraulic conductivity of binary sand-clay mixtures. One can refer to the procedure after Vu-Bac *et al.*, (2016) for a more comprehensive uncertainty analysis.

8. Conclusions

In this paper, the permeability behavior of remolded sand-marine clay mixtures is investigated, considering both the influence of the sand fraction and the initial water content. A simple model is proposed for the estimation of the overall hydraulic conductivity of the sand-clay mixtures using homogenization approach. The following conclusions are drawn:

(1) At a given stress level, the overall hydraulic conductivity is affected by both the sand fraction and the initial water content. This is due to the fact that a sample with a higher initial water content possesses a higher void ratio at the same consolidation stress.

(2) After being plotted in terms of (overall) hydraulic conductivity and (overall) void ratio on a double-logarithmic (ln*e*-ln*k*) scale, the influence of the initial water content on the overall hydraulic conductivity of seems to be negligible.

(3) A simple model is proposed using the homogenization approach. It has four parameters: two intrinsic and two structure ones, respectively. The model can well reproduce the permeability behavior of both the sand-marine clay mixtures in this study and the one from literature.

Acknowledgement

The work in this paper is supported by a National State Key Project “973” grant (Grant No.: 2014CB047000) (sub-project No. 2014CB047001) from Ministry of Science and Technology of the People’s Republic of China, a CRF project (Grant No.: PolyU12/CRF/13E) from Research Grants Council (RGC) of Hong Kong Special Administrative Region Government of China.

References

Barla, M., & Beer, G. (2012). Special issue on advances in modeling rock engineering problems. International Journal of Geomechanics, 12 (6), 617-617.

Bian, X., Wang, Z. F., Ding, G. Q., & Cao, Y. P. (2016). Compressibility of cemented dredged clay at high water content with super-absorbent polymer. *Engineering Geology*, 208, 198-205.

Bian, X., Cao, Y. P., Wang, Z. F., Ding, G. Q., & Lei, G. H. (2017). Effect of super-absorbent polymer on the undrained shear behavior of cemented dredged clay with high water content. Journal of Materials in Civil Engineering, 29(7).

British Standards Institution (1991). Methods of test for soils for civil engineering purposes, *BS 1377*. BSI, Milton Keynes.

Budarapu, P. R., Gracie, R., Yang, S. W., Zhuang, X., & Rabczuk, T. (2014). Efficient coarse graining in multiscale modeling of fracture. *Theoretical and Applied Fracture Mechanics*, 69, 126-143.

Butterfield, R. (1979). A natural compression law for soils (an advance on e-$\log p'$). *Géotechnique*, 29(4).

Carrier, W. D., & Beckman, J. F. (1984). Correlations between index tests and the properties of remoulded clays. *Géotechnique*, 34(2), 211-228.

Cerato, A. B., & Lutenegger, A. J. (2004). Determining intrinsic compressibility of fine-grained soils. *Journal of Geotechnical and Geoenvironmental Engineering*, 130(8), 872-877.

Chu, J., & Leong, W. K. (2002). Effect of fines on instability behavior of loose sand.

Géotechnique, 52(10), 751-755.

Deng, Y., Wu, Z., Cui, Y., Liu, S., & Wang, Q. (2017). Sand fraction effect on hydro-mechanical behavior of sand-clay mixture. *Applied Clay Science*, 135, 355-361.

Elkady, T. Y., Shaker, A. A., & Dhowain, A. W. (2015). Shear strengths and volume changes of sand-attapulgite clay mixtures. Bulletin of Engineering Geology and the Environment, 74(2), 595-609.

Eshelby, J. D. (1957). The determination of the elastic field of an ellipsoidal inclusion, and related problems. In *Proceedings of the Royal Society of London A: Mathematical, Physical and Engineering Sciences*, 241, 376-396.

González, C., & LLorca, J. (2000). A self-consistent approach to the elasto-plastic behaviour of two-phase materials including damage. *Journal of the Mechanics and Physics of Solids*, 48(4), 675-692.

Graham, J., Saadat, F., Gray, M. N., Dixon, D. A., & Zhang, Q. Y. (1989). Strength and volume change behavior of a sand-bentonite mixture. *Canadian Geotechnical Journal*, 26(2), 292-305.

Hashin, Z. (1983). Analysis of composite materials. *Journal of Applied Mechanics*, 50(2), 481-505.

He, B., Mortazavi, B., Zhuang, X., & Rabczuk, T. (2016). Modeling Kapitza resistance of two-phase composite material. *Composite Structures*, 152, 939-946.

Herle, I., & Gudehus, G. (1999). Determination of parameters of a hypoplastic constitutive model from properties of grain assemblies. *Mechanics of Cohesive-frictional Materials*, 4(5), 461-486.

Hill, R. (1965). A self-consistent mechanics of composite materials. *Journal of the Mechanics and Physics of Solids*, 13(4), 213-222.

Hong, Z., & Onitsuka, K. (1998). A method of correcting yield stress and compression index of Ariake clays for sample disturbance. *Soils and foundations*, 38(2), 211-222.

Hong, Z., Yin, J., & Cui, Y. J. (2010). Compression behavior of reconstituted soils at high initial water contents. *Géotechnique*, 60(9), 691-700.

Hong, Z. S., Zeng, L. L., Cui, Y. J., Cai, Y. Q., & Lin, C. (2012). Compression behavior of natural and reconstituted clays. *Géotechnique*, 62(4), 291.

Huang, L., Tan, L., & Zheng, W. (2016). Renovated Comprehensive Multilevel Evaluation Approach to Self-Healing of Asphalt Mixtures. *International Journal of Geomechanics*, 16(1).

Jamei, M., Villard, P., & Guiras, H. (2013). Shear failure criterion based on experimental and modeling results for fiber-reinforced clay. *International Journal of Geomechanics*, 13(6), 882-893.

Kumar, G. V. (1996). Some aspects of the mechanical behavior of mixtures of kaolin and coarse sand (*Doctoral dissertation, University of Glasgow*).

Lielens, G., Pirotte, P., Couniot, A., Dupret, F., & Keunings, R. (1998). Prediction of thermo-mechanical properties for compression moulded composites. *Composites Part A: Applied Science and Manufacturing*, 29(1), 63-70.

Mashiri, M. S., Vinod, J. S., & Sheikh, M. N. (2016). Constitutive model for sand-tire chip mixture. *International Journal of Geomechanics*, 16(1).

Mesri, G., & Olson, R. E. (1971). Mechanisms controlling the permeability of clays. *Clays* *and Clay Minerals*, 19(1), 151-158.

Mitchell, J. K. 1993, Fundamentals of Soil Behavior, John Wiley and Sons, Inc., New York.

Monkul, M. M., & Ozden, G. (2005). Effect of intergranular void ratio on one-dimensional compression behavior. In *Proceedings of International Conference on Problematic Soils*, International Society of Soil Mechanics and Geotechnical Engineering, Famagusta, Turkish Republic of Northern Cyprus (Vol. 3, pp. 1203-1209).

Mori, T., & Tanaka, K. (1973). Average stress in matrix and average elastic energy of materials with misfitting inclusions. *Acta Metallurgica*, 21(5), 571-574.

Pandian, N. S., Nagaraj, T. S., & Raju, P. N. (1995). Permeability and compressibility behavior of bentonite-sand / soil mixes. *Geotechnical Testing Journal*, 18(1), 86-93

Quayum, M. S., Zhuang, X., & Rabczuk, T. (2015). Computational model generation and RVE design of self-healing concrete. *Frontiers of Structural and Civil Engineering*, 9(4), 383-396.

Reuss, A. (1929). Berechnung der Fliessgrenzen von Mischkristallen auf Grund der Plastizitatsbedingung fuer Einkristalle, *Zeitschrift fuer angewandte Mathematik und Mechanik* 9, 49-58.

Shi, X. S., & Herle, I. (2015). Compression and undrained shear strength of remoulded clay mixtures. *Géotechnique Letters*, 5(2), 62-67.

Shi, X. S. & Herle, I. (2017). Numerical simulation of lumpy soils using a hypoplastic model. *Acta Geotechnica* 12(2), 349-363.

Shi, X. S., Herle, I., & Muir Wood, D. (2017). A consolidation model for lumpy composite soils in open-pit mining. *Géotechnique*, 1-16.

Silva, S. D. Three runway system project (3RS project), contract 3206 – main reclamation works. *Report for ZHECC-CCCC-CDC joint venture*. 7076481/R00: Hong Kong, 2016.

Sivapullaiah, P. V., Sridharan, A., & Stalin, V. K. (2000). Hydraulic conductivity of bentonite-sand mixtures. *Canadian Geotechnical Journal*, 37(2), 406-413.

Sridharan, A. & Prakash, K. (1996). Discussion on 'interpretation of oedometer test data for natural clays.' *Soils and Foundations* 36(3), 146-148.

Sridharan, A., & Prakash, K. (2003). Self-weight consolidation: compressibility behavior of segregated and homogeneous fine-grained sediments. *Marine Georesources and Geotechnology*, 21(2), 73-80.

Talebi, H., Silani, M., Bordas, S. P., Kerfriden, P., & Rabczuk, T. (2014). A computational library for multiscale modeling of material failure. *Computational Mechanics*, 53(5), 1047-1071.

Tan, T. S., Yong, K. Y., Leong, E. C., and Lee, S. L. (1990). Behavior of clay slurry. *Soils and Foundations*, 30(4), 105-118.

Thevanayagam, S., & Mohan, S. (1998). Intergranular void ratio-steady state strength relations for silty sands. In *Geotechnical Earthquake Engineering and Soil Dynamics III*: (pp. 349-360). ASCE.

Tsuchida, T. (2017). $e\text{-}\log\sigma_v$ relationship for marine clays considering initial water content to evaluate soil structure. *Marine Georesources & Geotechnology*, 35(1), 104-119.

Tu, S. T., Cai, W. Z., Yin, Y., & Ling, X. (2005). Numerical simulation of saturation behavior of physical properties in composites with randomly distributed second-phase. *Journal of composite materials*, 39(7), 617-631.

Voigt, W. (1928). Lehrbuch Der Kristallphysik, *Teubner Verlag*, Berlin-Leipzig.

Vu-Bac, N., Lahmer, T., Zhuang, X., Nguyen-Thoi, T., & Rabczuk, T. (2016). A software framework for probabilistic sensitivity analysis for computationally expensive models. *Advances in Engineering Software*, 100, 19-31.

Watabe, Y., Yamada, K., & Saitoh, K. (2011). Hydraulic conductivity and compressibility of mixtures of Nagoya clay with sand or bentonite. *Géotechnique*, 61(3), 211-219.

Weibull, W. (1951), A statistical distribution function of wide applicability. *Journal of Applied Mechanics. ASME*, 18 (3): 293-297.

Zeng, L. L., Hong, Z. S., Cai, Y. Q., & Han, J. (2011). Change of hydraulic conductivity during compression of undisturbed and remolded clays. *Applied Clay Science*, 51(1), 86-93.

Zeng, L. L., Hong, Z. S., & Chen, F. Q. (2012). A law of change in permeability coefficient during compression of remolded clays. *Rock and Soil Mechanics*, 5, 001.

Zeng, L. L., Hong, Z. S., & Cui, Y. J. (2015). Determining the virgin compression lines of reconstituted clays at different initial water contents. *Canadian Geotechnical Journal*, 52(9), 1408-1415.

Zeng, L. L., Hong, Z. S., & Gao, Y. F. (2016). Practical estimation of compression behaviour of dredged clays with three physical parameters. *Engineering Geology*.

Zhang, J., & Yang, J. (2017). Experimental and Numerical Investigation of Dilation Behavior of Asphalt Mixture. *International Journal of Geomechanics*, 17(2).

Zhou, Z., Yang, H., Wang, X., & Liu, B. (2017). Model Development and Experimental Verification for Permeability Coefficient of Soil–Rock Mixture. *International Journal of Geomechanics*, 17(4).

Zhuang, X., Huang, R., Liang, C., & Rabczuk, T. (2014). A coupled thermo-hydro-mechanical model of jointed hard rock for compressed air energy storage. *Mathematical Problems in Engineering*, 2014.

Zhuang, X., Wang, Q., & Zhu, H. (2015). A 3D computational homogenization model for porous material and parameters identification. *Computational Materials Science*, 96, 536-548.

Zhuang, X., Wang, Q., & Zhu, H. (2017). Effective properties of composites with periodic random packing of ellipsoids. *Materials*, 10(2), 112.

List of Tables

Table 1: Basic physical properties of the tested materials

Material	Liquid limit	Plastic limit	Density of particles	Sand	Silt	Clay
—	(%)	(%)	(Mg/m^3)	(%)	(%)	(%)
Clay	62.4	27.5	2.68	0	85	15
Sand	—	—	2.63	100	0	0

Table 2: Parameters for estimating the permeability of the sand-clay mixtures

Clay matrix	Sand inclusions	A_c	ξ_c	α	β	References
—	—	(cm/s)	(cm/s)	—	—	—
HKMD	Coarse sands	-18.25	4.35	0.74	0.70	This study
Bentonite	Fine sands	-29.65	6.73	0.77	0.73	Pandian *et al*., 1995
90%Bentonite+10%Kaolin	Poorly-graded sands	-26.62	4.50	0.70	0.68	Deng *et al*., 2017
70%Bentonite+30%Kaolin	Poorly-graded sands	-25.31	4.17	0.70	0.68	Deng *et al*., 2017
50%Bentonite+50%Kaolin	Poorly-graded sands	-23.41	3.52	0.70	0.68	Deng *et al*., 2017
Nagoya clay	Well-graded sands	-18.39	3.65	0.50	0.33	Watabe *et al*., 2011
Bentonite	Coarse sands	-24.17	3.57	0.70	0.60	Sivapullaiah *et al*., 2000
Bentonite	Fine sands	-24.17	3.57	0.70	0.62	Sivapullaiah *et al*., 2000

List of Figures

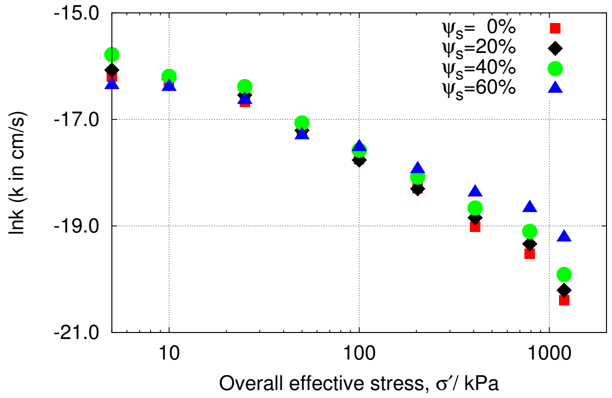

(a) w_{c0} = 67.9 %

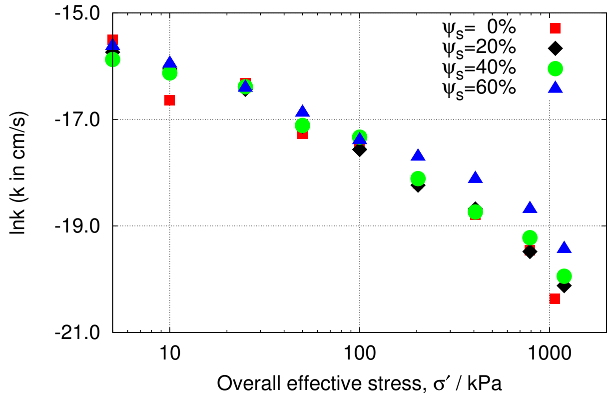

(b) w_{c0} = 74.5 %

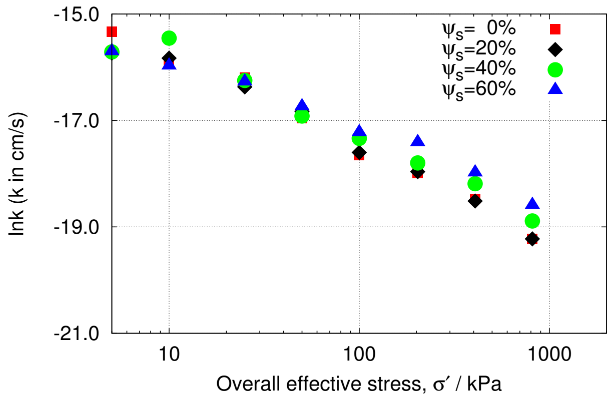

(c) w_{c0} = 86.9 %

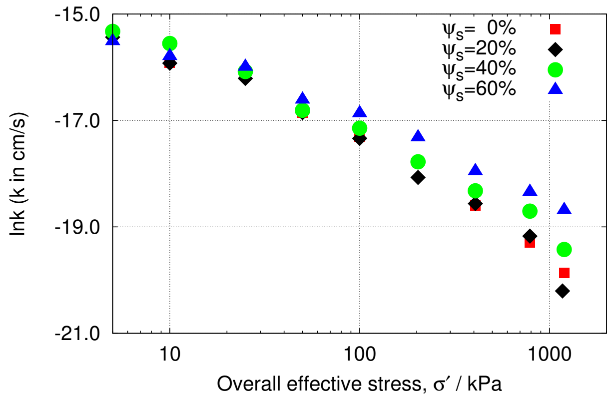

(d) w_{c0} = 99.5 %

Figure 1: Change of permeability of sand-marine clay mixtures (or pure clay) with increasing stress level

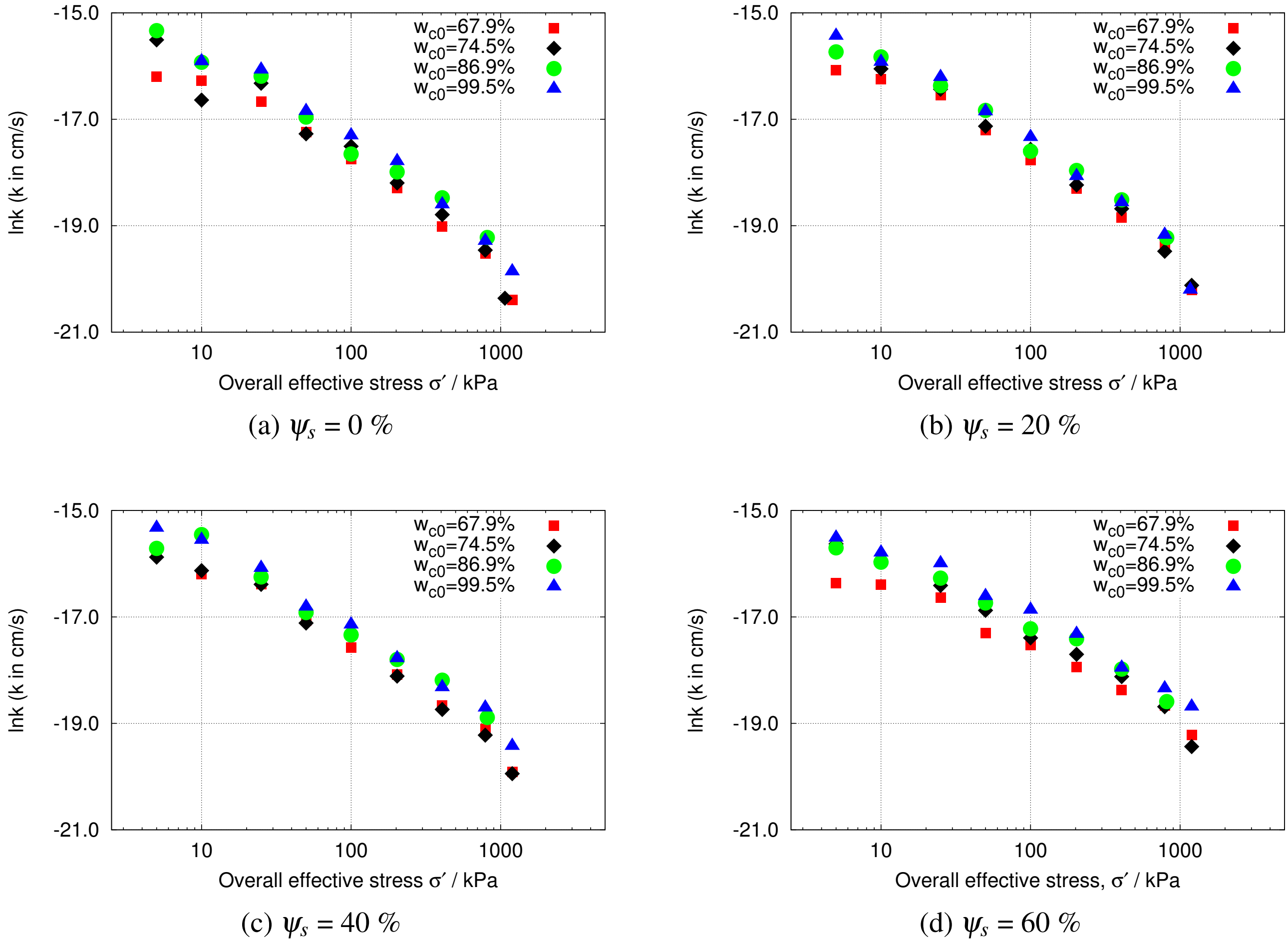

(a) $\psi_s = 0$ %

(b) $\psi_s = 20$ %

(c) $\psi_s = 40$ %

(d) $\psi_s = 60$ %

Figure 2: Effect of initial water contents of clay matrix on the overall permeability

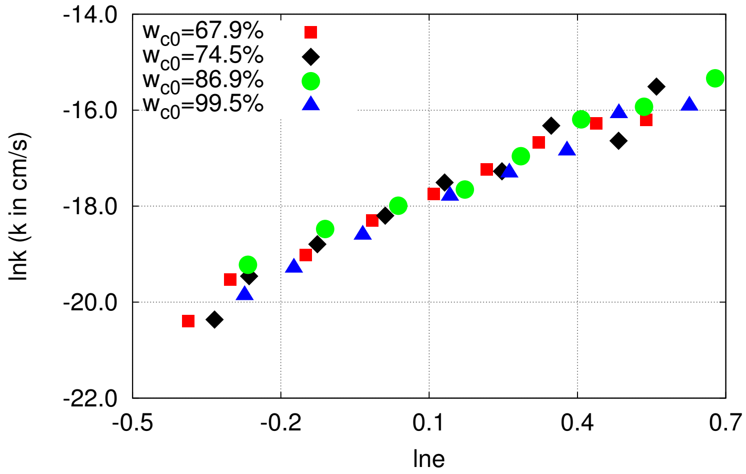

(a) Pure marine clay

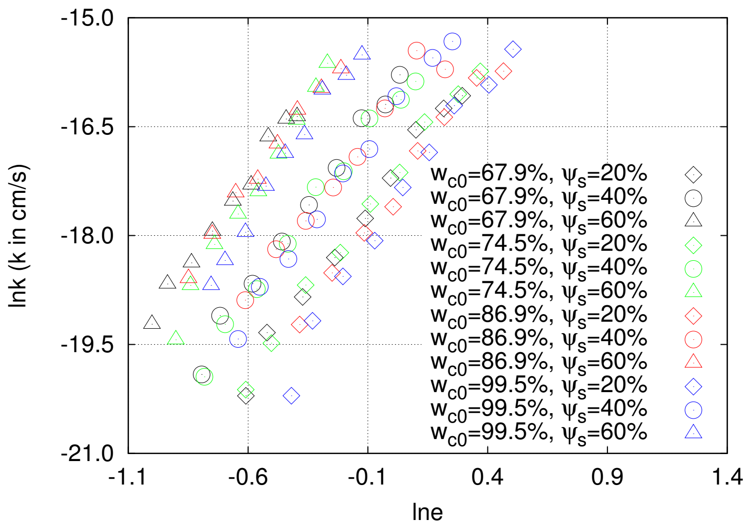

(b) Sand-marine clay mixtures

Figure 3: Permeability vs. void ratio relationship for pure marine clay and sand-clay mixtures

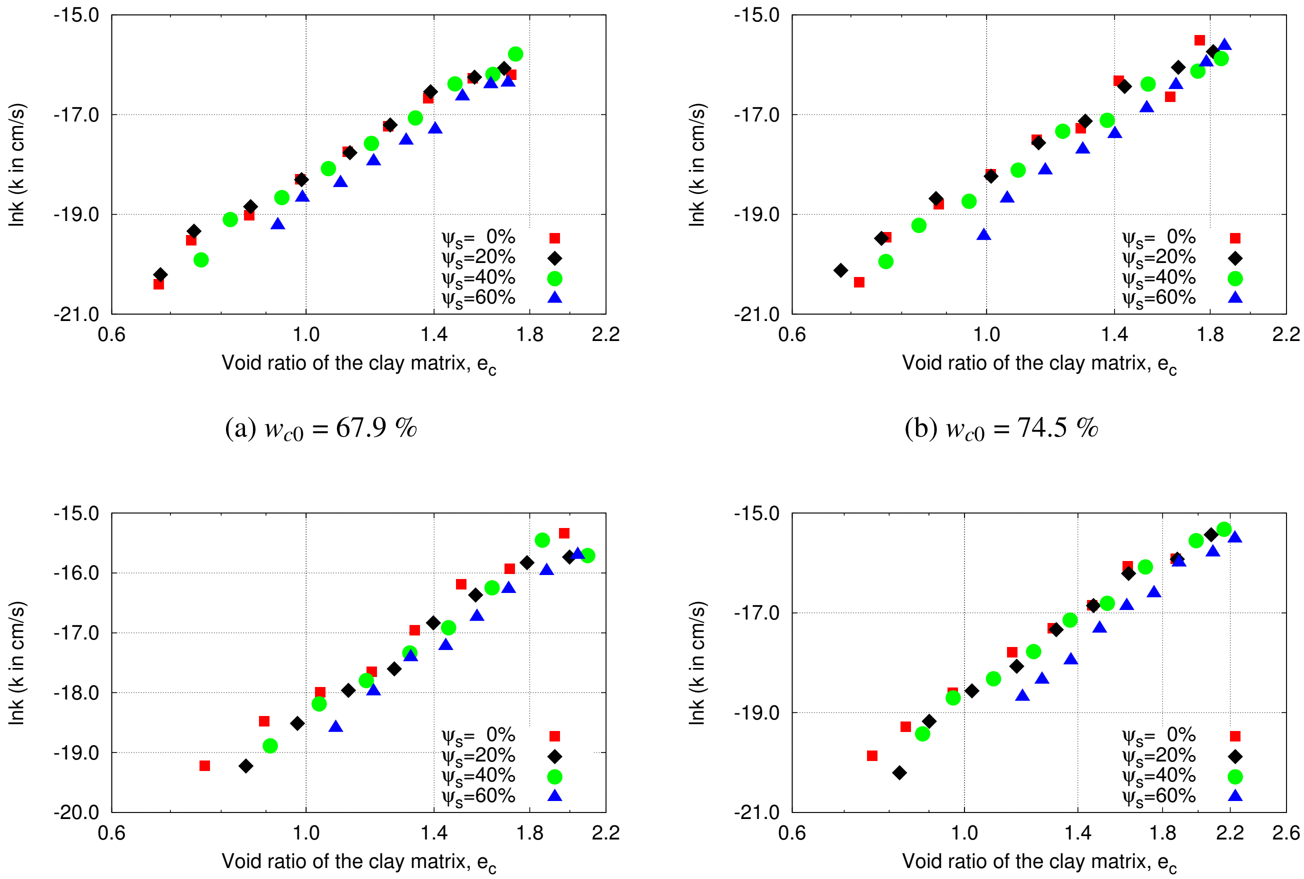

(a) w_{c0} = 67.9 %

(b) w_{c0} = 74.5 %

(c) w_{c0} = 86.9 %

(d) w_{c0} = 99.5 %

Figure 4: Relationship between the local porosity of the clay matrix and the overall permeability

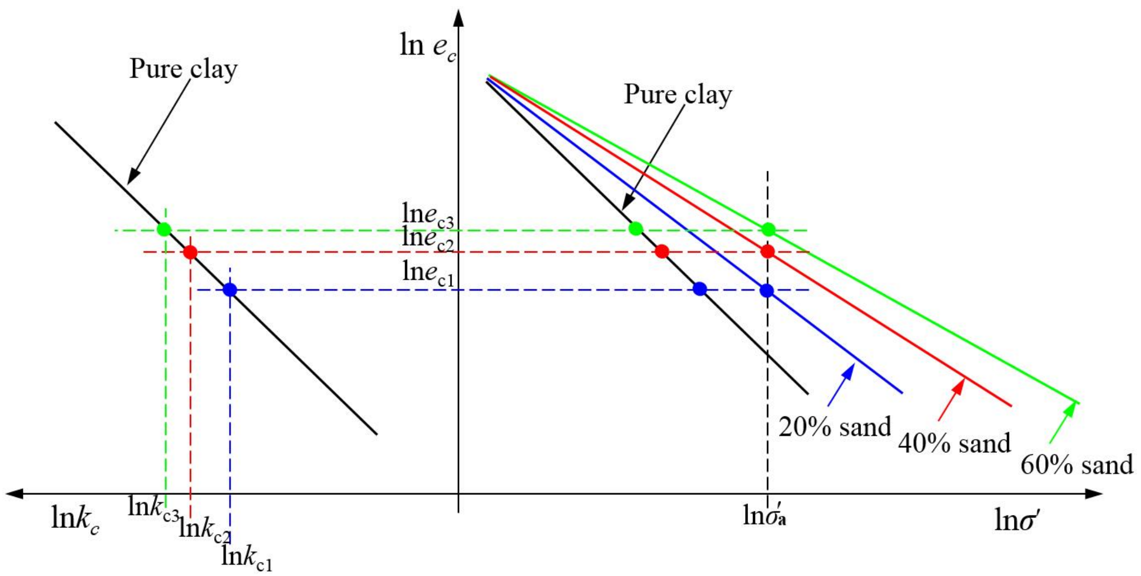

Figure 5: Schemetric plot for the calculation of the local variables in remolded sand-clay mixtures

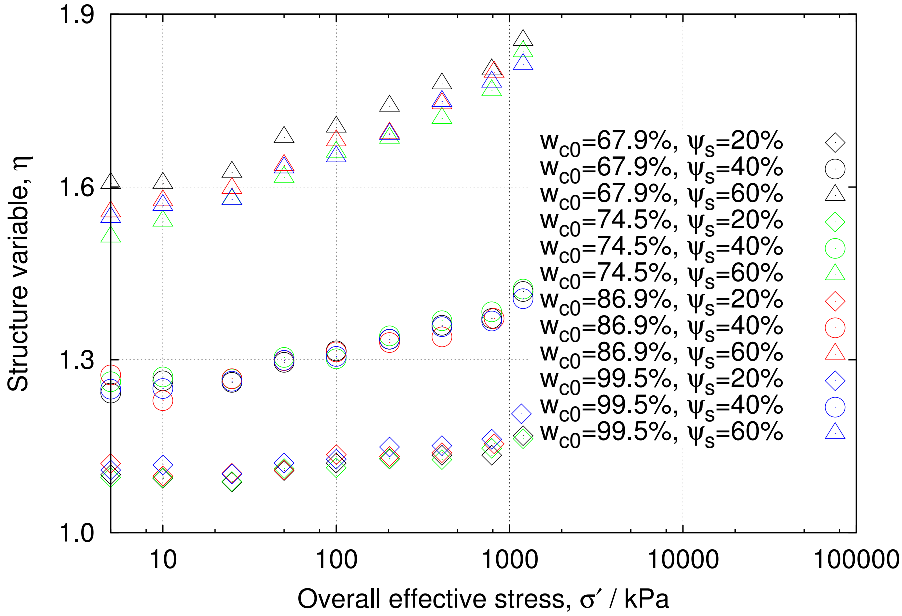

Figure 6: Evolution of structure variable η with increase of the stress level

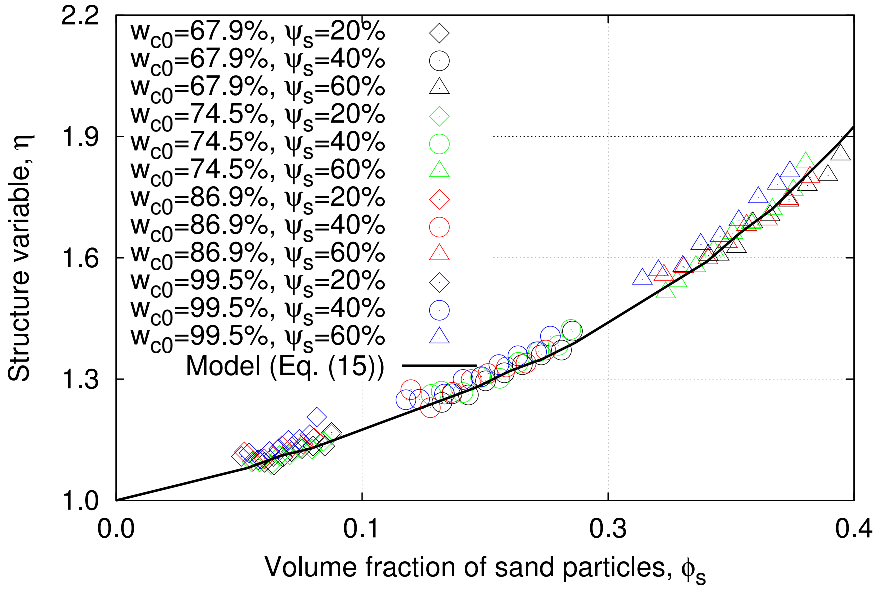

Figure 7: Evolution of structure variable η with volume fraction of sand particles

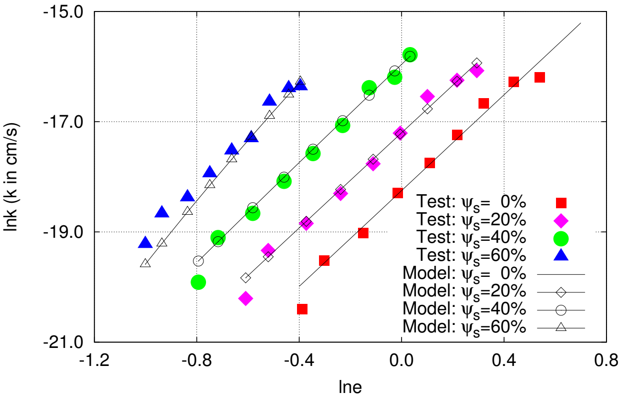

(a) w_{c0} = 67.9 %

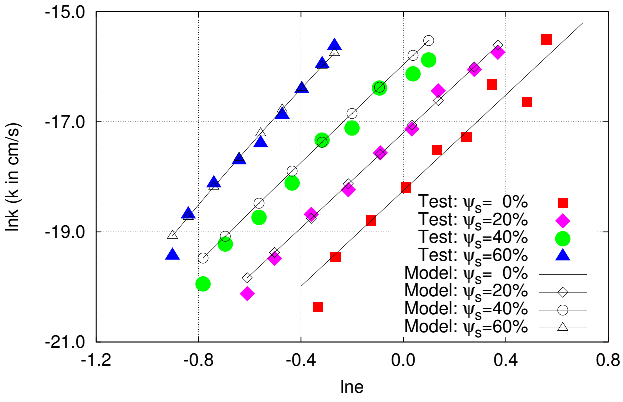

(b) w_{c0} = 74.5 %

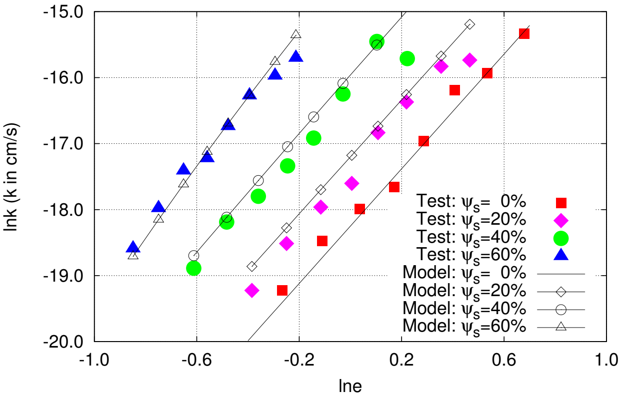

(c) w_{c0} = 86.9 %

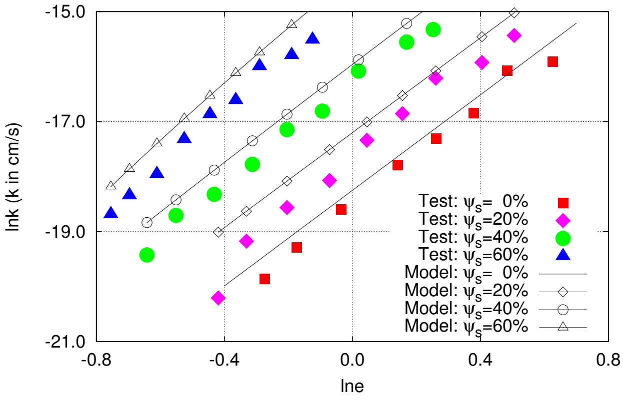

(d) w_{c0} = 99.5 %

Figure 8: Comparison between the model prediction and the experimental data

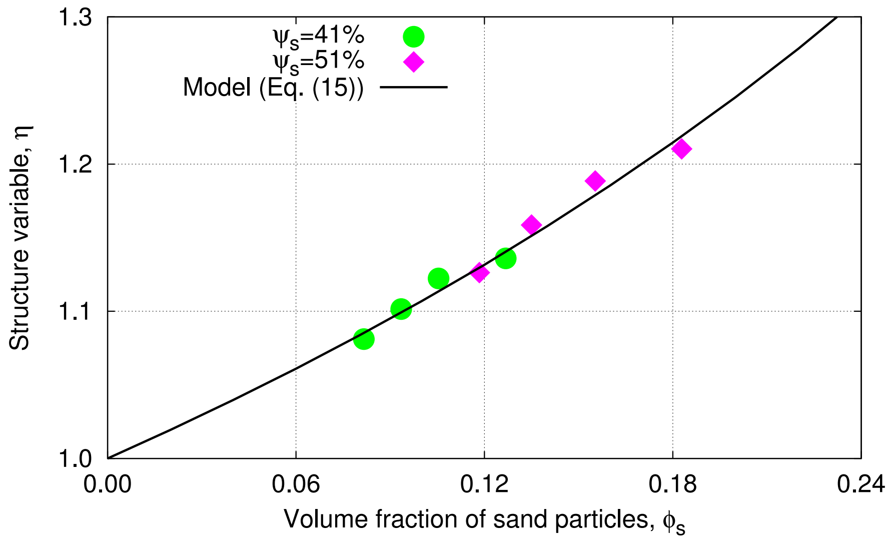

Figure 9: Change of structure variable η with volume fraction of sand particles

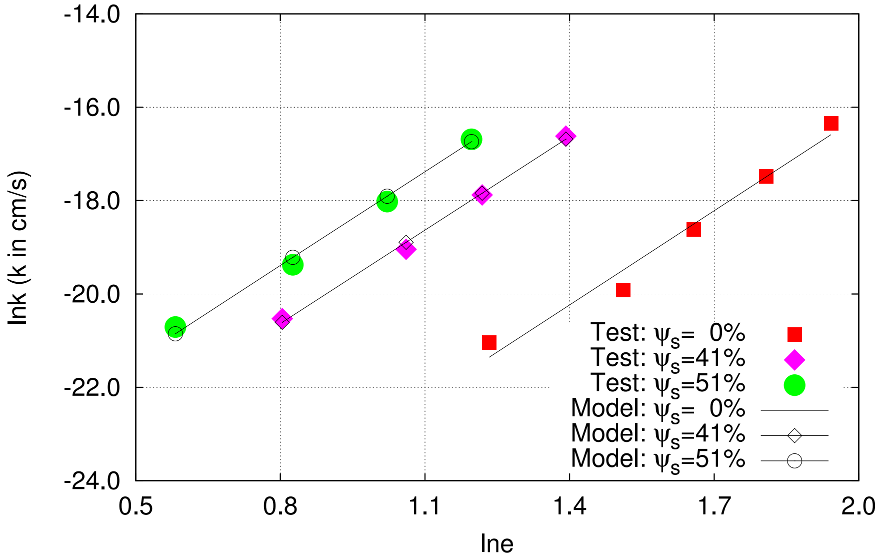

Figure 10: Comparisons between the experimental data and theoretical simulations

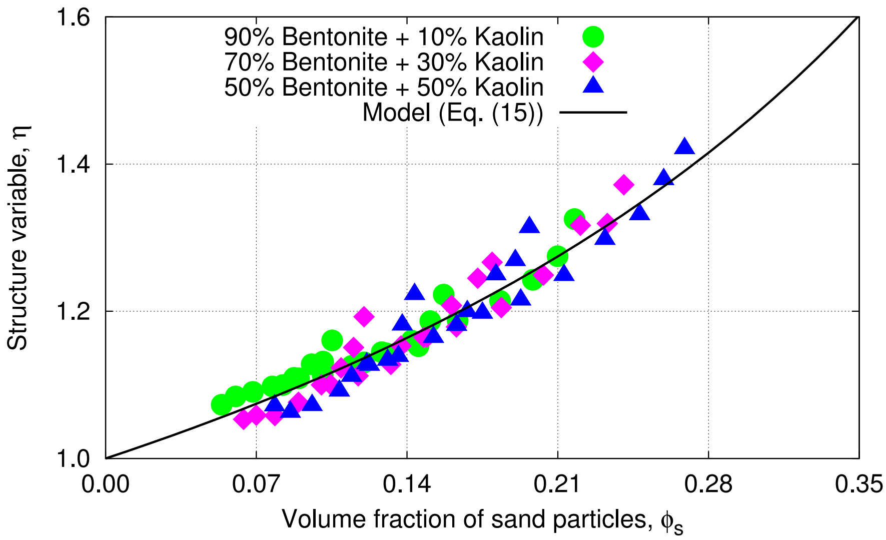

Figure 11: Change of structure variable η with volume fraction of sand particles

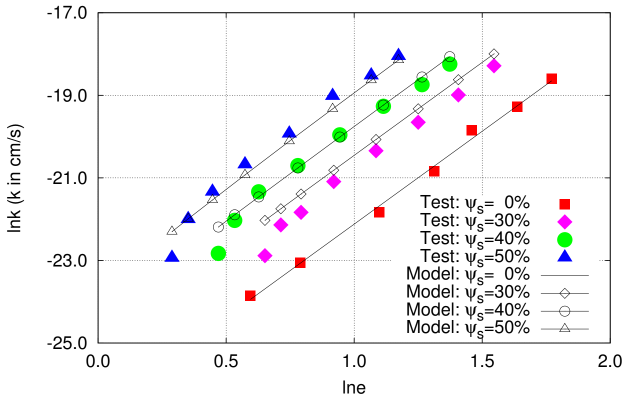

(a) 90% Bentonite+ 10% Kaolin

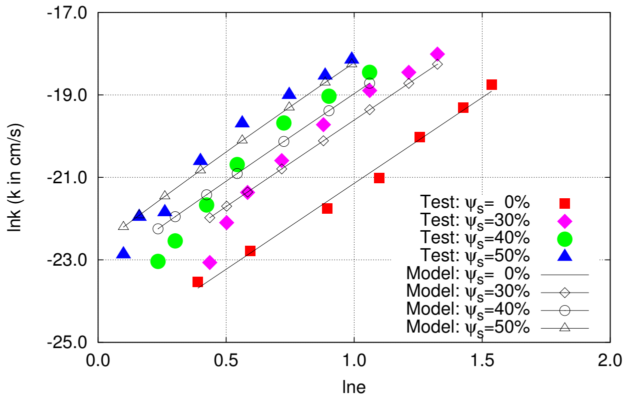

(b) 70% Bentonite+ 30% Kaolin

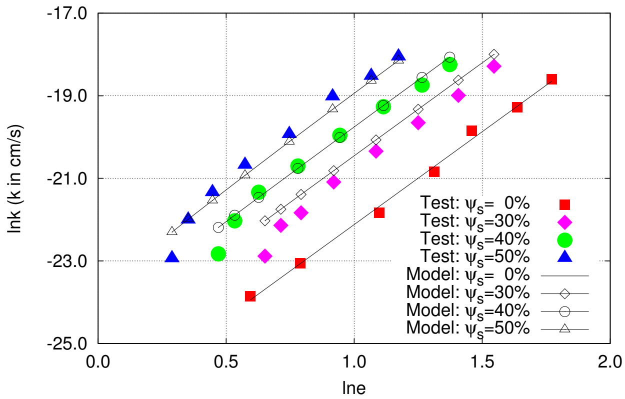

(c) 50% Bentonite+ 50% Kaolin

Figure 12: Comparison between the model prediction and the experimental data

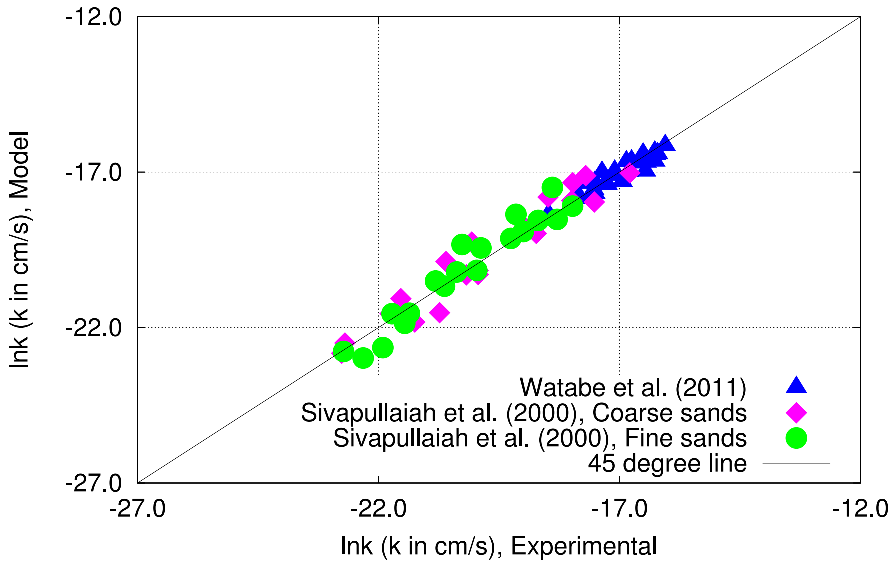

Figure 13: Comparison between the experimental values and model predictions